UNIVERSITY OF TARTU
FACULTY OF SCIENCE AND TECHNOLOGY
INSTITUTE OF MOLECULAR AND CELL BIOLOGY

Maare Mõttus

Development of new plant F-actin reporters by a split-tagging system

Bachelor thesis

Supervisor
Yuh-Shuh Wang

TARTU 2015

TABLE OF CONTENTS

ABBREVIATIONS **3**

INTRODUCTION **4**

1. LITERATURE OVERVIEW **5**

1.1. The actin cytoskeleton **5**

1.2. Visualizing the actin cytoskeleton **5**

1.3. Advancements in live cell fluorescent imaging by fusion of multiple fluorescent proteins **7**

1.4. Advancements in live cell imaging by a protein tagging system based on antibody-antigen interaction **8**

2. EXPERIMENTAL PART **10**

2.1. Aims of current study **10**

2.2. Materials **11**

2.2.1. Media and chemicals 12

2.2.2. Bacterial strains and plant line 12

2.3. Methods **12**

2.3.1. Preparation of competent cells 12

2.3.2. Transformation and colony-PCR 13

2.3.3. Traditional cloning method 14

2.3.4. Modified Golden Gate cloning method 15

2.3.5. Amplification by overlapping-PCR 15

2.3.6. Agro-infiltration 16

2.3.7. Live cell imaging 17

RESULTS **18**

3.1. Molecular cloning of class I constructs **19**

3.1.2. Multimerization of PDZ fragment by using different cloning methods. **19**

3.2. Molecular cloning of class II constructs **20**

3.2.1. Signal peptide and GFP-PDZlig-myc fragment insertion into the pCAM1390 vector under the 35S promoter. 20

3.3. Actin filaments imaging in agro-infiltrated *Nicotiana benthamiana* **21**

3.3.1. Effects of different promoters 21

3.3.2. Quality control for class II constructs 22

3.3.3. Live cell imaging by co-infiltration of class I and class II constructs 23

3.3.4. Our imaging strategy is time sensitive 25

3.3.5. Current approach requires further optimization to increase fluorescence signal 26

3.3.6. mCherry effects on actin live imaging 27

DISCUSSION **28**

SUMMARY **31**

KOKKUVÕTE **32**

LITERATURE CITED **34**

Used web addresses **36**

SUPPLEMENTS **37**

1. Restriction enzymes **37**

ABBREVIATIONS

ABD – actin binding domain

ABP – actin binding protein

bp – base pair

dpi – day post infiltration

F-actin – filamentous form of actin, consisting of globular actin monomers

G-actin – monomeric globular form of actin, which polymerizes form actin filaments (F-actin)

GFP – green fluorescent protein

RE – restriction endonuclease

SP – signal peptide

SP^{NLS} – nucleus localization signal peptide

SP^{Chl} – chloroplast localization signal peptide

INTRODUCTION

Actins are the most abundant globular proteins in eukaryotic cell, which are essential building units for actin filaments (F-actins). Via an accurately regulated processes F-actins form a filamentous network – actin cytoskeleton, which plays a primary role in vital cellular processes, like cell shape changing, cytokines, cytoplasmic streaming, and also intracellular signaling. Furthermore, it provides a platform for interacting with neighboring cells. Numerous actin-binding proteins (ABP) participate in determining the dynamics and configuration of actin cytoskeleton. To date, a large number of ABPs have been described, but mostly have been studied by biochemical assays *in vitro*, thus their functions in plants remain uncharacterized. Nevertheless, characterization of the actin cytoskeleton and ABP molecular functions has been a focus in plant cell biology.

Our understanding of actin dynamics and structures relies primarily on tools and techniques, which permit actin visualization of actin in living cells. Initially, most commonly used methods were performed in fixed materials labelled with fluorescently tagged phalloidin or by immunocytochemistry. Presently they have been predominantly replaced with a new class of live plant F-actin probes based on the green fluorescent protein (GFP). The major problem with GFP-based F-actin probes associates with disruptions in actin organization caused by overexpression of the actin-binding domain (ABD) of regulatory ABPs. Furthermore, the fluorescence signal from currently available F-actin reporters is frequently too weak to allow identification of certain fine and subtle structures. Therefore, there are still needs in the development for better reporters.

The aim of current study was to improve fluorescence imaging on the actin cytoskeleton by a split-tagging system, in which a synthetic protein scaffold was used to recruit multiple GFPs for fluorescence signal amplification.

Current study was performed in The Plant Signal Research Group at the Institute of Technology. I would like to thank Yuh-Shuh Wang, who was creative and inspiring supervisor and in addition all helpful members from our research group.

1. LITERATURE OVERVIEW

1.1. The actin cytoskeleton

Actins are abundant and highly conserved globular proteins in eukaryotes. They are mainly located in cytoplasm, but are also present in the nucleus, where they may or may not have motor-associated functions (Remedios et al., 2002). Under certain physiological conditions actin monomers (G-actin) assemble into polar, helical filamentous structures (F-actin), which have two biochemically and structurally distinct ends called barbed end and pointed end. ATP-dependent polymerization in barbed end and depolymerization in pointed end cause filaments treadmilling, which plays a decisive role in actin-based motile processes (Pantaloni et al., 2001; Bugyi et al., 2010). The F-actin is the basic building unit for actin cytoskeleton complex network, which is highly dynamic and can undergo rapid changes upon various stimuli. Numerous actin-binding proteins and small molecules play essential roles in modulating the dynamics of the actin cytoskeleton (Kreplak et al., 2007; Dominiquez et al., 2011).

Actin cytoskeleton drives indispensable processes for normal cell growth and development. For example, F-actin facilitates the maintenance of the internal architecture of the cell, drives cytoplasmic streaming, contributes to the process of cell division and provides a platform for interaction with neighboring cells (Remedios et al., 2002; Hussey et al., 2006; Kreplak et al., 2007; Deeks et al., 2009, McKayed et al., 2013). Furthermore, actin cytoskeleton provides trafficking routes for delivery of cell wall precursor containing vesicles to the site of polarized growth and functions as molecular tracks, which guide intracellular movements in response to environmental stimuli (Drøbak et al., 2004). Not less important are actin-mediated signaling cascades, which dictate the plant protection strategies against pathogens and facilitate response to abiotic stresses (Dyachok et al., 2014; Nick, 1999). Consequently, as actin cytoskeleton provides several fundamental functions in the cell, it has been an important research field in cell biology. As tools and techniques that allow us to visualize actin are central to our understanding towards actin biology. The race of inventing and improving different methods has been continuous and been accelerateing in the past quarter of a century (McKayed et al., 2013).

1.2. Visualizing the actin cytoskeleton

The past two decades have been an explosion in development of new techniques in cell biology, especially in the field of light microscopy and imaging (Blancaflor, et al 2000). Originally F-actin was only observed in fixed materials by immunolabelling (immunofluorescence) or using

fluorophores conjugated to the actin binding drug phalloidin (Krauss et al., 2003; Deeks et al., 2009). These approaches have contributed to our understanding of how the plant cytoskeleton is reorganized during cell cycle and in response to various environmental stimuli (Lloyd et al., 1987; Blancaflor et al., 2000; Collings et al., 2005). However, as plant samples often required prolonged chemical fixation and permeabilization treatments, these methods are prone to generating artifacts (Schnell et al., 2012). In addition, only static images could be obtained, which makes it impossible or difficult on studies of the actin dynamics.

In the nineties, more dynamic elements, such as fluorescently labelled phalloidins, were introduced through microinjection in living plant cells for imaging purpose. This technique allowed visualization of two F-actin populations that were not co-localized, of which one presumably was newly assembled during cell plate development after microinjection (Schmit et al., 1990). Alternatively, in the nineties, fluorescent analogs of actins were injected into cytoplasm of living plant cells, by which the cytoskeleton structure that maintains nuclei in a centralized position was reported (Ren et al., 1997). The critical nuance of microinjection was that it was time-consuming, required accurate technical expertise and specialized equipment, and it could perturb cellular processes. Since the discovery of the green fluorescent protein (GFP) and identification of its gene, the visualization of protein dynamics and gene expression in living cells has evolved tremendously. GFP appeared to be the ideal genetically encoded *in vivo* reporter due to its low toxicity to the cell and high sensitivity that enables easy detection with fluorescence microscope (Chalfie et al., 1994). Introduction of GFP heralded a new class of live plant cytoskeleton probes, thus the actin imaging in plants spread widely and has become routine in many laboratories (Kost et al., 1998, Timmers et al., 2002; Genove., et al 2005).

Fluorescent probes are normally fusion proteins of a GFP (or its variants) and a protein that specifically targets to the site or structure of interest. For example, the first invented cytoskeletal fluorescent probe was GFP-MBD (GFP fusion to the microtubule-binding domain of microtubule-associated protein 4), through which the microtubule organization was accurately described in living cells (Marc et al., 1998). Similarly, the GFP-Talin (actin-binding domain of talin) and GFP-ABD2 (actin-binding domain 2 of fimbrin 1) were used in F-actin organization imaging (Kost et al., 1998; Wang et al., 2004). Altogether these genetically encoded F-actin reporters allow further comprehensive and extensive studies on plant actin biology. They have helped to increase our understanding on actin functions in cell polarity establishment, organelle dynamics, and plant virus movement (Ketelaar et al., 2004; Sheahan et al., 2004; Liu et al., 2005; Sano et al., 2005). However, widened use of fluorescent probes has revealed some issues concerning side-effects. For example, plant growth defects caused by perturbed actin

organization and dynamics have been reported. In addition, loss of fluorescence due to gene silencing has been a common phenomenon, especially when the reporters were driven by a strong constitutive promoter. In many cases, both problems could be overcome by using a weaker promoter. However, low expression levels of the live reporters often lead to weak fluorescent signals, which make imaging difficult (Wang et al., 2004, Ketelaar et al., 2004; Wang et al., 2008).

Requirement for fluorescent signal amplification in imaging process is driving constant development of new methods, which allow better visualization with minimal side-effects. Significant progress has been made by multimerization of fluorescent proteins.

1.3. Advancements in live cell fluorescent imaging by fusion of multiple fluorescent proteins

It has been shown that fluorescent signal intensity could be increased by protein multimerization (Wang et al., 2008). Several attempts have been made to use fluorescent proteins as reporters of promoter activity, hitherto with limited success. The main reason may lie in the low activities of most promoter. Therefore the yield of fluorescent protein is not sufficient for visualization without antibody enhancement (Fleischmann et al., 1998). It has been demonstrated that by improving the spectral yield of fluorescent protein the signal can be enhanced (Gong et al., 2003). However, engineering of the fluorescent proteins requires specialized expertise. On the other hand, fluorescence output after in-frame multimerization of up to three copies of fluorescent protein monomers increased signal intensity proportionally, whereas construct with 6 copies of fluorescent protein displayed weaker signals than the three copy construct. This was likely caused by instabilities of repeated DNA sequences and proteins of tandem repeats (Genové et al., 2005).

To increase fluorescent signals for actin imaging, an additional GFP tag was added to the ABD2-GFP reporter, which resulted in significant improvement on the fluorescence output (Wang et al., 2008). By using this live actin reporter, researchers have gained insights on how the root hair polarity is established (Yoo et al., 2012). Major problems of fluorescent protein-based F-actin probes in plants associate with perturbed actin organization and growth defects. These effects have been reported for every F-actin markers during their development. Several researches have shown that F-actin binding GFP probes inhibit the growth of plants or some cell types, for instance the GFP-ABD2-GFP reporter has a minor inhibitory effects to the growth of cells and tissues of young *Arabidopsis* seedlings. Furthermore, the F-actin binding GFP reporters often cause partial or total loss of fluorescence, especially in the root meristem

and elongation zone (Sheahan et al., 2004; Wang et al., 2004; Wang et al., 2008; Dyachok et al., 2014). Minor improvement in minimizing mentioned side-effects has been made by using the moderate ubiquitin 10 promoter (pUBQ10) instead of the strong constitutive 35S promoter (p35S) from the cauliflower mosaic virus (Norris et al., 1993; Wang et al., 2008; Dyachok et al., 2014).

Altogether, several studies have shown that addition of up to 3 copies of extra GPF molecules could increase fluorescence spectral yield for protein localization or gene expression studies (Genové et al., 2005; Wang et al., 2008, Dyachok et al., 2014). However, fusion with more than 3 copies of fluorescent protein has been technically challenging and has failed to increase fluorescent signals so far. For more efficient use of live actin reporters, it is important to further increase signal-to-noise ratio that allows imaging under lower expression levels of the ABD2 domain to minimize perturbation of the native structures.

1.4. Advancements in live cell imaging by a protein tagging system based on antibody-antigen interaction.

Very recently, a novel protein tagging system, named the SunTag (SUperNova), was reported to achieve tagging with up to 24 copies of GFP in the live cell reporters (Tanenbaum et al., 2014). The principle of SunTag system lies on interaction between antibodies and antigens. Instead of direct fusion to a fluorescent protein, the protein of interest was tagged with multiple repeats of short peptide, which in turn recruited multiple copies of GFP fused to a specific antibody fragment that recognized the peptide (Figure 1). Using the SunTag system, fluorescence signals increased dramatically, which allowed single molecule imaging with a regular confocal microscope. In addition, the strong signal-to-noise ratio of the SunTag allowed easy imaging even when the tagged protein was expressed at very low levels. For example, the fluorescence signal of $SunTag_{24x}$ with plasma membrane targeting domain in the C terminus was 18-fold brighter than the single GFP fused to the same targeting domain.

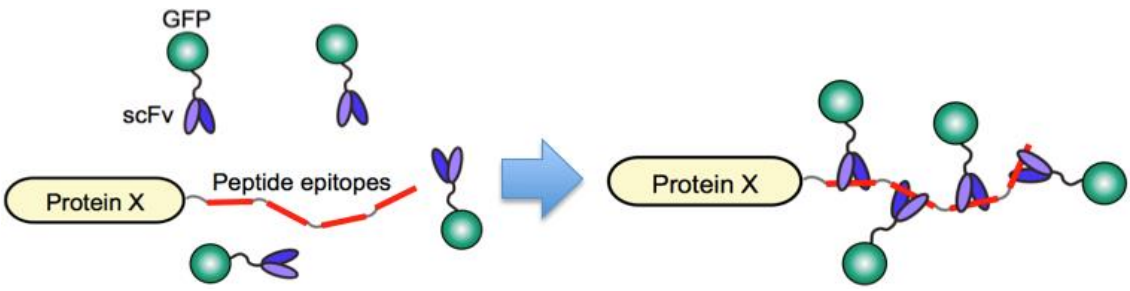

Figure 1. Schematic of the antibody-peptide labelling method for the SunTag system **(Tanenbaum et al., 2014). (**Antibodies were marked violet)

Antibody based systems have several advantages, including their very high affinity and ability to recognize short peptides. However, main issues of antibody-based systems, including the SunTag system lies in the relatively large size of antibodies and low expression levels and limited solubility in the cell (Tanenbaum et al., 2014).

Alternative to antibody based methods, is the use of well-defined protein-protein interaction modules. Dueber and co-workers have reported a synthetic protein scaffold approach to recruit various and multiple enzymes in a spatially designed manner. The protein scaffold was composed of various copies of three small protein-protein interaction domains. Various enzymes were tagged with the corresponding ligands, which bind to the specific domains. The synthetic scaffold in turn guided enzymes tagged with ligands to form a multi-enzyme complex that resembled the natural metabolon (Dueber et al., 2009). A large number of protein-protein interaction module pairs have been well characterized, and many of them are small enough as potential protein tags (Binz et al., 2004). Therefore, modifications of the SunTag system with small protein-protein interaction modules represent opportunities for developing new actin reporters for live imaging in plants.

2. EXPERIMENTAL PART

2.1. Aims of current study

A number of actin reporters have been developed for live cell imaging, and their usage has provided valuable insights on the structure, dynamics and functions of the actin cytoskeleton. Despite their usefulness, current live actin reporters still possess certain limitations, such as weak fluorescence or undesired side-effects due to perturbance of the actin structure and dynamics.

Thus, the main goal of current study was to develop new actin reporters using a modified SunTag system. The specific aims include:

- To generate new constructs using various molecular cloning techniques
- To evaluate new constructs as potential actin reporters in transient assays by agro-infiltration and confocal microscopy.

2.2. Materials

All plasmids used or created in current study are shown in the Table 1.

Table 1. Used or created plasmids

Plasmid name	Characterization	Reference
PDZ-SH3lig-HA	In vector pUC57-Mini	Genes are synthesized by GenScript
HisStrp-SH3-PDZlig myc	In vector pUC57-simple, size 2710 bp	Genes are synthezised by GenScript
p35S/pCAM1390		Wang et al., 2004
p35S:GFP-ABD2-GFP		Wang et al., 2008
pUBQ10:GFP-ABD2-GFP		Dyachok et al., 2014
pUBQ10:mCherry-ABD2-mCherry		Dyachok et al., 2014
pICH78133	5'UTR,(Tobacco Mosaic Virus)+chloroplast transit peptide, RbcS (syntetic)	Golden Gate Plant Parts Kit, Engler et al., 2014
pAGM5331	5'UTR, (Tobacco Mosaic Virus, nuclear localization signal (Simian Virus 40)	Golden Gate Plans Parts Kit, Engler et al., 2014
p35S:GFP-PDZlig	In vector pCAM1390	This study, class II construct
p35S:SP^{Chl}-GFP-PDZlig	In vector pCAM1390	This study, class II construct
p35S:SP^{NLS}-GFP-PDZlig	In vector pCAM1390	This study, class II construct
pUBQ10:ABD2-3xPDZ	In vector pCAM1390	This study, class I construct
pUBQ10:ABD2-4xPDZ	In vector pCAM1390	This study, class I construct
pUBQ10:ABD2-4xPDZ-6xHis	In vector pCAM1390	This study, class I construct
pUBQ10:ABD2-5xPDZ	In vector pCAM1390	This study, class I construct
pUBQ10:ABD2-5xPDZ-6xHis	In vector pCAM1390	This study, class I construct

2.2.1. Media and chemicals

LB medium and LB agar used for growing bacteria were form Difco. Ticarcillin disodium and kanamycin was purchased from Duchefa Biochemie.

All components for digestion reaction (fast digest restriction enzymes, 10X fast digest buffer), ligation reaction (T4 DNA ligase, 10X T4 DNA ligase buffer) and some components for PCR amplification (10x DreamTaq buffer, 10mM ATP) were manufactured by Thermo Scientific. DNA polymerase Taq FirePol was manufactured by Solis Biodyne and GeneRuler by Fermentas.

2.2.2. Bacterial strains and plant line

Escherichia coli strain **DH5α** was used for maintaining and purification of plasmid DNA. ***Agrobacterium tumefaciens*** strain **C58_GV3101** was used for immobilizing constructs into tobacco plant leaves by agro-infiltration method. **Tobacco** plant line ***Nicotiana benthamiana*** was used as a host for agrobacterium with established constructs.

2.3. Methods

2.3.1. Preparation of competent cells

Preparation of *Escherichia coli* strain DH5α competent cells by TSS method

The *E. coli* cells were grown in 3ml of LB media at 37°C overnight. One ml of overnight culture was added into 50ml fresh LB in a 250ml flask and cultured for about 3 hours at 37°C, until OD_{600} reached to 0.4. The bacterial culture was then incubated on ice for 30 minutes and subsequently pelleted at 4,000 rpm for 5 minutes at 4°C. TSS solution containing 10% PEG 8000, 50mM $MgCl_2$, 5% DMSO in LB was prepared previously by filter sterilization and stored at 4°C. Pelleted bacterial cells were gently resuspended in 5ml of ice-cold TSS solution on ice, and aliquoted to 90μl per tube. All aliquots of competent cells were placed to liquid nitrogen for snap-freezing and stored at -80°C.

Preparation of *Agrobacterium tumefaciens* strain C58_GV3101 competent cells

The single colonies of *A. tumefaciens* were grown in 3ml LB media with 100mg/L gentamycin overnight at 28°C shaker at 200 rpm. The overnight culture was inoculated in 50ml LB with gentamycin and incubated in 28°C until OD_{600} was 0.5. After measurement the culture was chilled on ice for 10 minutes and subsequently centrifuged at 4,000 rpm for 10 minutes at 4°C.

The cells were resuspended in 10ml of ice-cold 0.15M NaCl and centrifuged for 10 minutes at 4,000 rpm at 4°C. Pellet was resuspended in 5ml of 20mM ice-cold $CaCl_2$. The competent cells were aliquoted in 50µl per tube, snap-frozen in liquid nitrogen and stored at -80°C.

2.3.2. Transformation and colony-PCR

E. coli transformation was performed by heat shock method, by which 30µl competent *E. coli* cells were added to ligation mixture with gentle mixing. The mixture was incubated on ice for 20 minutes, and transported into the water bath for heat shock (at 42°C for 90 seconds). After heat shock the mixture was transported to ice for 3 minutes immediately. Transformed cells were incubated with gentle shaking (200 rpm) in 300µl LB at 37°C for 1 hour. After incubation, 200µl of mixture was plated on selective LB plates, containing appropriate antibiotic – 80mg/L Ticarcillin disodium or 50mg/L kanamycin, according to the specifics of used vector. Plates were incubated upside-down at 37°C overnight.

Similarly, *agrobacterium* transformation was performed by heat shock method. About 500ng of plasmid DNA was added to 50µl of frozen *agrobacterium* competent cells, and incubated at 37°C for 10 minutes. 300µl of LB was added after heat shock, and the cells were incubated at 28°C for 1-2 hours. 200µl of transformation mixture was plated on LB plates with 50mg/L kanamycin, and incubated at 28°C for 2-3 days.

After transformation, colonies were verified by colony-PCR, using ESCO (Peltier Tehnology TAS) Aeris or Professional Thermocycler machine. One colony was touched and pipetted into 6,4µl water in the PCR tube, subsequently 13,6µl master mixture was added. The final PCR reactions included 250nM each of forward and reverse primers, 1X DreamTaq polymerase buffer, 200µM dNTPs, 0.2µl Taq DNA polymerase (FirePol 5U/µl, Solis Biodyne). PCR program included three different phases, firstly 30 second initial denaturation at 95°C. Second phase contained 30 cycles for amplifying a specific DNA sequence. One cycle consisted of three successive steps, 15 second denaturation at 95°C, 15 second annealing at 55°C and about 1min/kb for elongation at 72°C. The incomplete PCR fragments were allowed to elongate by additional elongation step at 72°C for 5 minutes.

The size of PCR products was verified by electrophoresis in 1% agarose gel, with GelGreen Nucleic Acid stain (Biotium). The Labnet Gel_{XL} Ultra V-2 gel bath filled (approximately 300ml) with 0,5xTBE buffer (89mM Tris base, 89mM boric acid, 2 mM EDTA for 1xTBE) was used. DNA fragments were viewed in a blue LED transilluminator (Clare Chemical Research) and documented in a gel-doc system (Cleaver Scientific Ltd). The size of DNA

fragments were evaluated by comparing them with DNA ladder (GeneRuler 1kb, Fermentas).

Colonies with right insert size were grown overnight in 5ml LB medium with Ticarcillin disodium or kanamycin, according to the antibiotic resistance gene in the vector. Plasmids were extracted from overnight cultures using FavorPrep Plasmid Extraction Mini Kit (Favorgen) according to manufacturer's protocol.

2.3.3. Traditional cloning method

The plasmid containing the synthetic PDZ domain was used in two separate digestion reactions. In one reaction the DNA was digested with BglII and XbaI REs for releasing PDZ fragment and in the other reaction the DNA was digested with BamHI and XbaI for preparation of the vector.

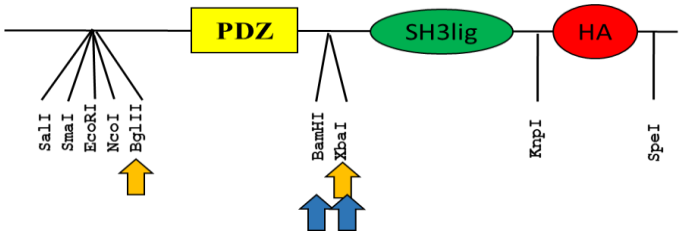

Figure 2. Creation of insert and vector. Orange arrows show insert restriction sites and blue arrows indicate vector restriction sites.

The digested vector and insert were purified by gel purification using a PCR/gel purification kit (Favorgen) according to manufacturer's protocol. The purified vector and insert were ligated together by T4 DNA ligase (Thermo Scientific) in 10µl ligation reaction containing 1X ligase buffer, and 0.5µl of T4 DNA ligase (5U/µl, Thermo Scientific). Ligation was carried out at room temperature for 30min followed by transformation into the competent *E.coli* cells. In the subsequent cloning steps, the construct containing 2xPDZ was used to prepare 2xPDZ insert and vector with 2xPDZ in a similar way to generate constructs with 4xPDZ. By combining different vectors and inserts, various tandem repeats of PDZ could be generated in the pUC57-mini backbone. However, the maxima number of PDZ in the pUC57-mini was only three. The 3xPDZ was then released by EcoRI and BamHI, and cloned into p35S/pCAMBIA1390 at the EcoRI/BglII site (XbaI and SpeI are isocaudomers). To create more than 3xPDZ constructs in the p35S/pCAMBIA1390 backbone, two types of PDZ inserts were digested by either EcoRI/BamHI or BglII/XbaI, and together cloned into p35S/pCAMBIA1390 at the EcoRI/SpeI site (XbaI and SpeI are isocaudomers). Subsequently, these constructs with various PDZ repeats in p35S/pCAMBIA1390 were used to generate the final class I constructs by cloning pUBQ10

(with HindIII/NcoI ends) and ABD2 (with NcoI/EcoRI ends) at the HindIII/EcoRI site. Similarly, the final assembly of class II constructs was carried out using the conventional cloning method with appropriate RE and ligation steps.

2.3.4. Modified Golden Gate cloning method

The PDZ fragment was released by two RE-s BglII and BamHI. Subsequently, in self-ligation in the presence of both REs, the fragments with multiple copies of PDZ was generated at 16˚C (Figure 2). The ligated BglII and BamHI ends cannot be recognized by either enzyme, whereas the undesired ligation products of BglII-BglII and BamHI-BamHI ends can be re-cleaved by the corresponding enzymes at 37˚C.

By alternating the incubation temperatures between 16˚C and 37˚C as described in the Golden Gate cloning method (Engler et al., 2008), various tandem PDZ copies in the head-to-tail configuration would be preferentially produced in the same reaction, resulting in different size ladders on the gel.

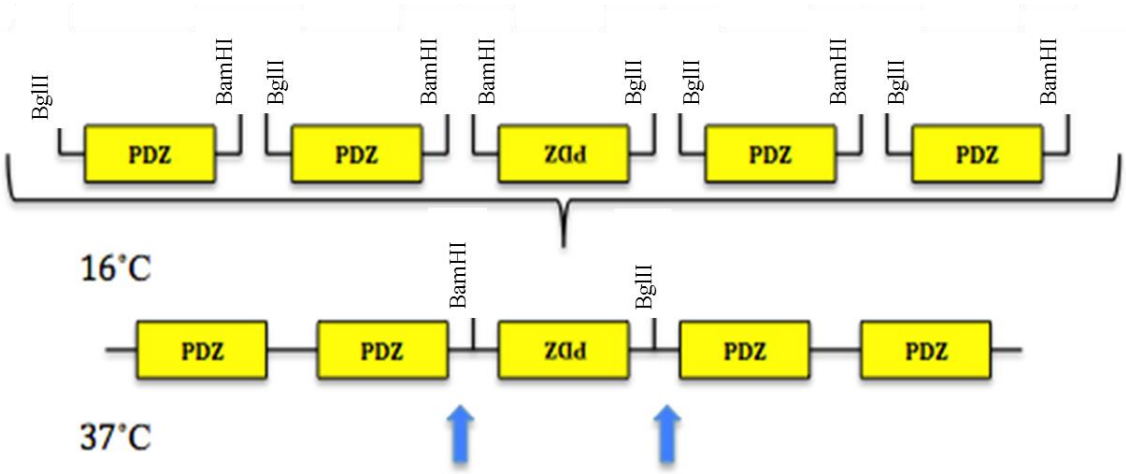

Figure 3. PDZ fragments assembling by a modified Golden Gate method. Plasmid DNA was digested with RE BglII and BamHI. Purified fragments were used in self-ligation reaction in the presence of both REs, with temperature alternating between 16˚C and 37˚C (Golden Gate protocol, Engler et al., 2009).

2.3.5. Amplification by overlapping-PCR

GFP-PDZlig fragment was prepared by two two-step-overlapping PCR cloning method (Figure 4). In the first reaction the GFP was amplified from template p35S:GFP-ABD2-GFP with the forward primer (EcoRI-YFP fwd: gagaattcatggtgagcaagggc) and reverse primer (GFP-Xlig R: tgatcctgaacctctcttgtacagctcgtc), and PDZlig from template HisStrp-SH3-PDZlig with forward

primer (GFP-Xlig F: gacgagctgtacaagagaggttcaggatca) and reverse primer (M13 R: ggaaacagctatgaccatg). These PCR products were mixed and used as the template for the subsequent PCR with EcoRI-YFP fwd and M13 R primers to amplify the GFP-PDZlig fragment.

The GFP-PDZlig was purified, digested by EcoRI and SpeI, and cloned into p35S/pCAMBIA1390 at the EcoRI/SpeI site. In addition, sequences of the nuclear and chloroplast-targeting signals were PCR-amplified, digested with SalI and EcoRI, and cloned into p35S:GFP-PDZlig/pCAMBIA1390 at the SalI/EcoRI site.

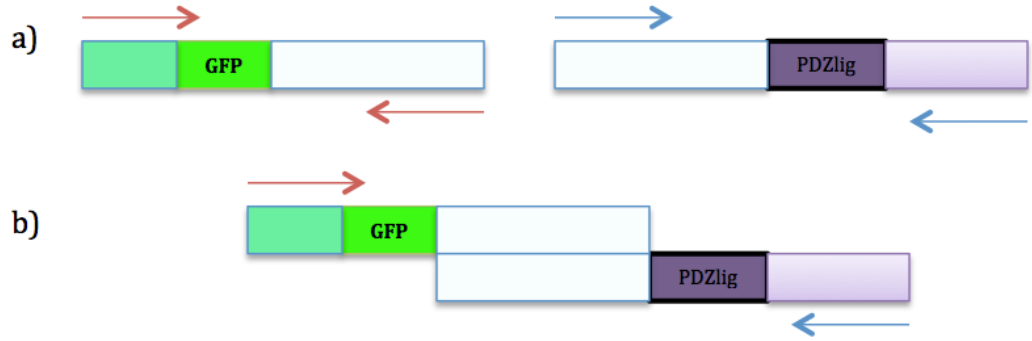

Figure 4. GFP-PDZlig amplification by overlapping-PCR. a) In the first round of PCR, both fragments – GFP and PDZlig were amplified separately. Primers were designed that 3' of the reverse primer for GFP is complementary to t5' of the forward primer for PDZlig. b) During the second PCR the complementary overlaps annealed and allows amplification for the entire GFP-PDZlig fragment by using the forward primer for GFP and reverse primer for PDZlig during the first round of PCR.

2.3.6. Agro-infiltration

Agro-infiltration experiments were performed on tobacco plant *Nicotiana benthamiana*. One single colony from each different transformed *A. tumefaciens* strain C58_GV3101 were cultured overnight at 28°C at 250 rpm in LB containing kanamycin (50mg/L) and gentamycin (100mg/L). The overnight culture was centrifuged at 28°C at 4000 rpm. Pellets were resuspended in infiltration buffer (10mM MgCl2; 10mM MES, 200 mM Acetosyringone) to OD_{600} of 0.6 (Ultraspec 10, Amersham Biosciences), and incubated at room temperature for 2 hours. Before infiltration, agrobacteria containing the specific constructs were mixed with additional *agrobacterium* carrying a gene silencing suppressor (P19). The final OD_{600} for each agrobacteria clone was 0.2. The final suspension was injected into the *Nicotiana benthamiana* leaves by using 1ml syringes (without the needles).

2.3.7. Live cell imaging

Selected leaves were cut 2 days post infiltration (dpi). The fluorescents signal was observed by stereo-microscopy equipped with an AxioCam MRc5 camera (SteREO Discovery.V20 Zeiss, objective PlanApoS 1,5x FWD 30mm). Infiltrated area was explored and the promising regions were marked for imaging with confocal-microscopy.

The confocal-microscope (Zeiss LSM710) was used for monitoring fluorescent signal in various layers of cell. Previously marked area was cut out with scalpel and placed with water between glass slide and cover glass. Prepared sample was observed with different objective (20x and 63x water). GFP was excited with 488nm laser, and mCherry was excited with 561nm laser. All confocal images were processed in Zeiss Zen 2011 Blue program.

RESULTS

The main goal of current thesis was test a new approach for actin cytoskeleton imaging in living plant cells via recruitment of multiple fluorescent proteins using a split-tagging system. This split-tagging system required two separate classes of constructs. Class I (Figure 1-a) contains an actin-binding domain (ABD) fused to various copies of a synthetic metazoan PDZ domain, a well-defined protein interaction module. Class II (Figure 1-b) are constructs of a green fluorescent protein (GFP) fused to the PDZ ligand (PDZlig), a short peptide that binds to the PDZ domain. Several cloning methods and concepts have been explored to generate the final constructs, which allows more flexible and effective cloning for the current project, as well as for future modifications.

After agro-infiltration in plant leaves, proteins from class I and class II constructs assemble by PDZ-PDZlig interaction. The ABD2 domain in the class I constructs would bind to F-actin, and the number of its PDZ fusions would determine how many copies of GFP being recruited to the new actin reporter complex. The intensity of fluorescent signal, in theory, would be proportional to the number of recruited GFPs (Figure 1-c).

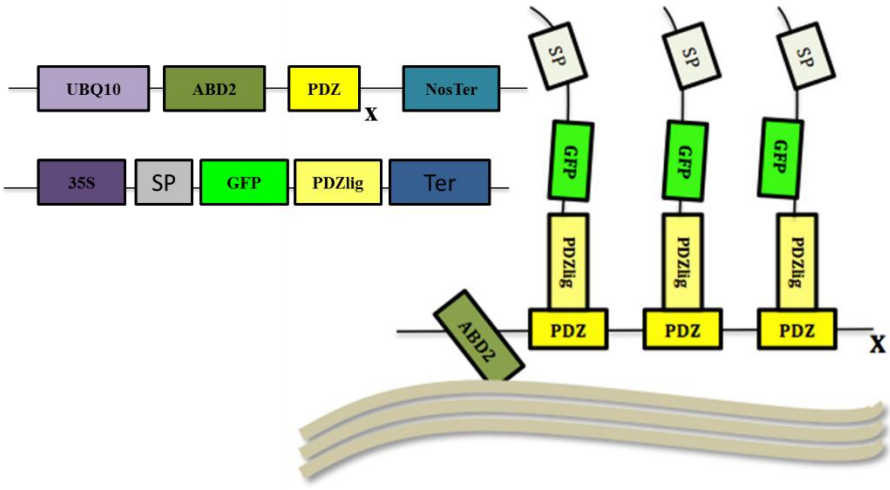

Figure 5. Class I and class II constructs and their incorporation. a) class I constructs consist a moderate promoter (Pro), actin binding domain ABD2, different copy numbers of PDZ (PDZ)x, and a terminator (NosTer); b) class II constructs consist of Pro, signal peptide (SP), fluorescent protein (GFP), the PDZ ligand (PDZlig, for binding to PDZ) and Ter; c) Fusion proteins from class I constructs bound to actin filaments via ABD2. The GFP-PDZlig from class II constructs interacts with PDZ, thus decorating the F-actin, whereas the unbound GFP-PDZlig is sequestered to specific organelle by the SP.

3.1. Molecular cloning of class I constructs

The main parts of the class I constructs are the actin-binding domain 2 (ABD2) of the *Arabidopsis* Fimbrin1 protein, and the synthetic PDZ domain. To minimize potential perturbation in the native structure and dynamics, these fusions need to be expressed at low to moderate levels. The *Arabidopsis* ubiquitin 10 promoter (pUBQ10), which drives gene expression constitutively at a moderate level was chosen for this study.

3.1.2. Multimerization of PDZ fragment by using different cloning methods.

As the first step, a synthetic construct containing the codon-optimized (for *Arabidopsis*) PDZ domain was ordered through a commercial gene synthesis service. This PDZ domain was designed to contain BglII and BamHI sites flanking the 5' and 3'-ends of the sequence, respectively. BglII and BamHI are isocaudomers that generate identical overhangs upon DNA cleavage (Supplemental 1), despite their slightly different recognition sites. We tried to create various copies of PDZ fragments in one step using the Golden Gate cloning concept (Engler et al., 2008). The purified PDZ fragments with complementary ends (BglII and BamHI) were incubated in a thermocycler. During cycles of alternating temperatures optimal for either ligase (16˚C) or restriction enzymes (37˚C), direct tandem repeats of PDZ would form preferentially, while avoiding the undesired ligation of inverted fragments. However, our first attempt only resulted in two direct PDZ repeats.

Alternatively, a more conventional stepwise approach was used, as described under in traditional cloning section in the Methods. First, we tried to multimerize PDZ domain in the small cloning vector, pUC57-mini, for ease of handling. However, despite several repeated experiments, the maximal number of PDZ genes in pUC57-mini was only three. Since the size of pUC57-mini is only 1835bp, we suspected that the insert size might be limited to 1kb, which is smaller than the size of 4xPDZ (about 1,2kb).

As multimerization of PDZ fragment (more than three) was unsuccessful in pUC-57mini, we performed further multimerization steps in another vector. The *Agrobacterium* binary vector pCAMBIA1390 (pCAM1390) with a kanamycin resistance gene was selected for further cloning, mostly because it was later applicable for plant transformation as well. In contrast to pUC57-mini, the pCAM1390 vector was larger (8861bp), and has been used to accommodate inserts of several kilo-base pairs previously. By using the conventional cloning methods, up to 5 copies of PDZ domain were introduced to the pCAM1390.

In addition to the PDZ domain, class I constructs also include the pUBQ10 and ABD2. The purified pUBQ10 and ABD2 fragments were cloned into the pCAM1390 containing various copies (3, 4, 5) of PDZ by 3-way ligation. Figure 6 showed the diagram of class I constructs generated and used for current study. All constructs were verified by sequencing and restriction enzyme digestion.

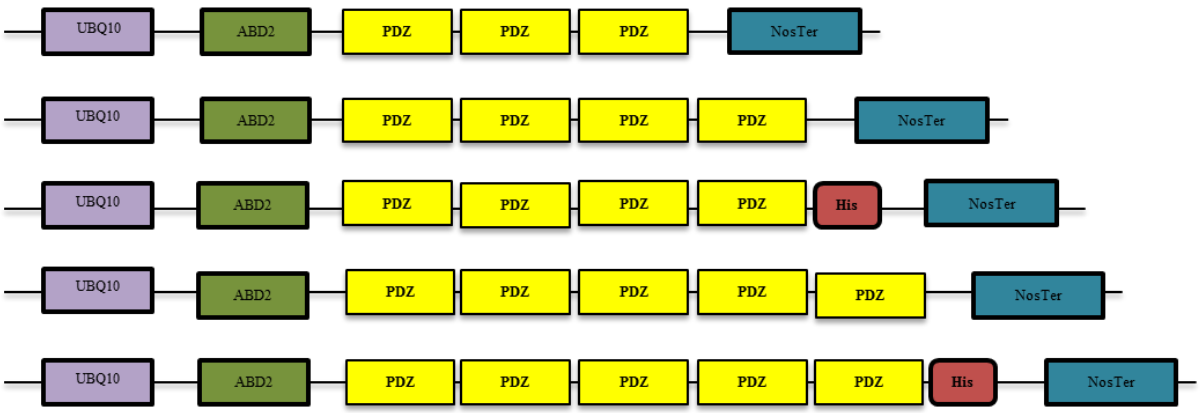

Figure 6. Diagram of all class I constructs generated in this study. All constructs are in pCAM1390.

3.2. Molecular cloning of class II constructs

The major components of class II constructs are coding regions of the green fluorescent protein (GFP) and the PDZ ligand (PDZlig). Ideally, these constructs need to be expressed at high levels, thus the strong constitutive 35S promoter (p35S) from cauliflower mosaic virus was chosen for this study. On the other hand, overexpression of the class II constructs may result in high background from unbound GFP-PDZlig fusions. Therefore, two additional constructs with signal peptides (SP) to the nucleus (NLS) or chloroplasts (Chl) fused to the GFP were generated to sequester unbound GFP to designated organelles.

3.2.1. Signal peptide and GFP-PDZlig-myc fragment insertion into the pCAM1390 vector under the 35S promoter.

The PDZlig is a small peptide of seven amino acids. DNA sequences encoding the PDZlig along with a c-myc epitope were designed and incorporated to other protein-protein interaction modules by a commercial DNA synthesis service. The c-myc epitope was included to aid future protein analysis with the anti-myc antibody. Due to the small size of the PDZlig and c-myc epitope (PDZlig-myc), we performed an overlap-PCR to create GFP fusions with PDZlig-myc, and cloned the GFP fusions into pCAM1390 under the control of p35S. In addition, sequences

of SP^{NLS} and SP^{Chl} were PCR-amplified, and added in-frame to the 5'-end of the GFP-PDZlig-myc fusion. Figure 7 showed the diagram of class II constructs created in this study.

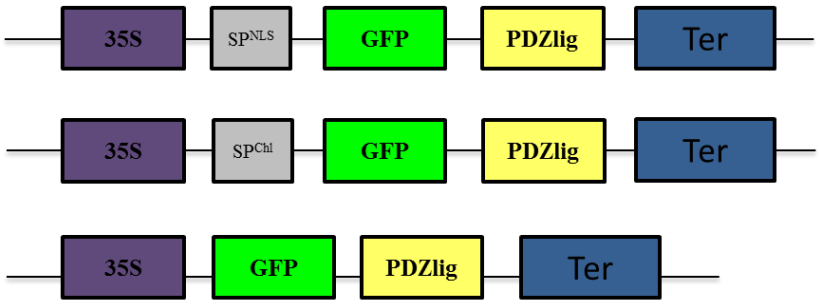

Figure 7. Diagram of all class II constructs used in this study. All constructs are in pCAM1390.

3.3. Actin filaments imaging in agro-infiltrated *Nicotiana benthamiana*

3.3.1. Effects of different promoters

As mentioned earlier, the selection of promoter was critical in establishing class I and class II constructs. To minimized disturbance to actin dynamics and its structure, class I constructs need to be expressed by a weaker promoter, whereas class II constructs require a strong promoter for fluorescence signal enhancement. In this study, we selected pUBQ10 as the weaker promoter, and p35S as the strong promoter. To compare the effects of these two promoters in the transient assays by agro-infiltration, we first tested two previously reported plant actin reporter constructs, the p35S:GFP-ABD2-GFP and pUBQ10:GFP-ABD2-GFP (Wang et al., 2008; Dyachok et al., 2014). As shown in Figure 8, p35S resulted in brighter signals under a wide field stereo-microscope. However, the signals from pUBQ10 appeared more uniform among transformed cells. Using a confocal microscope, both constructs gave very bright signals depicting the actin cytoskeleton.

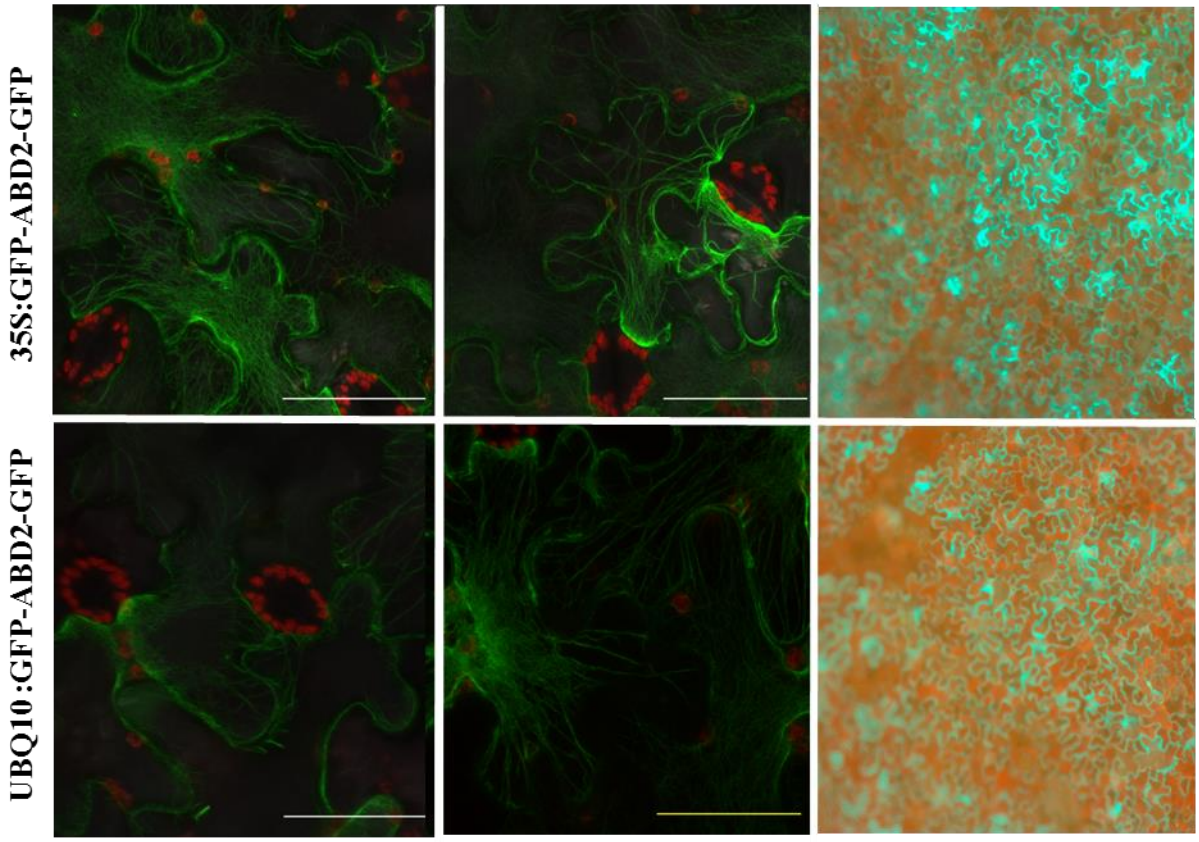

Figure 8. Comparison of 35S and UBQ10 promoters. Performed by using p35S:GFP-ABD2-GFP (Wang et al., 2008) (shown in the first row) and pUBQ10:GFP-ABD2-GFP (Dyachok et al., 2014) constructs (shown in the second row). Images from left and middle column were taken by confocal microscopy (63x-water objective). Right column images were taken by stereo-microscopy (1.5x objective). All images were taken on the 3rd day past infiltration. Scale bar = 50μm.

3.3.2. Quality control for class II constructs

The class II constructs functionality was verified by infiltrating separately without any class I construct. As expected, expression of p35S:SP^{NLS}GFP-PDZlig displayed fluorescence signals in the nucleus, whereas the SP^{Chl}GFP-PDZlig was located in chloroplasts. On the other hand, GFP-PDZlig without SP showed widely spread fluorescence signal in the cytosol and the nucleus. These results suggest that SP^{NLS} and SP^{Chl} have potential to sequester the cytosolic background caused by unbound class II fusions.

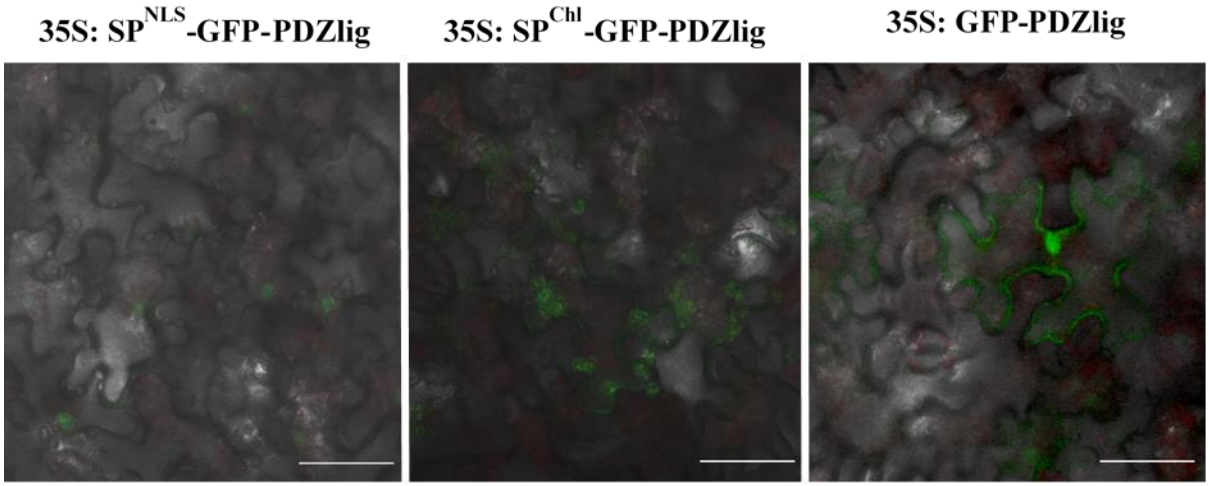

Figure 9. Sub-cellular localization of class II GFP fusions. SP^{NLS} and SP^{Chl} directed GFP-PDZlig to the nucleus (left) and chloroplasts (middle), respectively. The GFP-PDZlig without SP was found in the cytosol and the nucleus. All images were taken by confocal microscopy with 63x water objective. Scale bar = 50μm.

3.3.3. Live cell imaging by co-infiltration of class I and class II constructs

Each class I and class II construct was transformed into *Agrobacterium tumefaciens* separately. Tobacco leaves were co-infiltrated with two *Agrobacteria* clones each containing either class I or class II construct. During current study we established several class I constructs, out of which we selected three for co-infiltration experiments. All class II constructs passed the quality control and were used in co-infiltration assays. Nine possible combinations were made from three class I and three class II constructs.

We first monitored fluorescence on the 2^{nd} day post infiltration (dpi). As shown in the confocal images (Figure 10), the signal peptide had significant impact on the localization of fluorescence signal. Despite comprehensive screening we could not observe any distinct actin filaments in any of class I and class II combinations at 2 dpi time point.

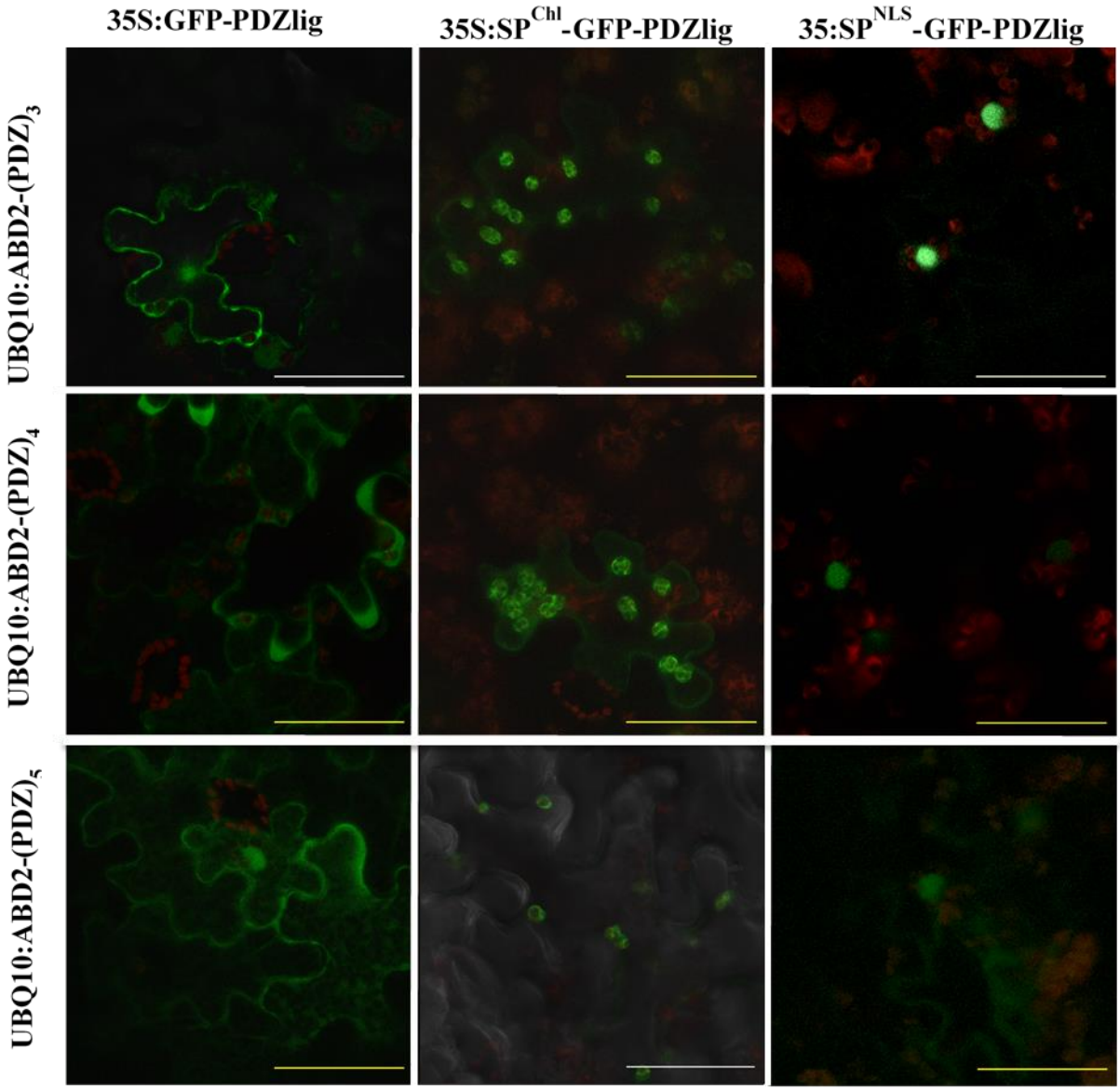

Figure 10. Confocal images of different combinations of class I and class II constructs on the 2nd dpi. Images of leaves co-infiltrated with class I (indicated in the left) and class II (indicated on top) constructs. All images were taken by confocal microscopy (63x water objective) on the second day after infiltration. Scale bar = 50μm.

3.3.4. Our imaging strategy is time sensitive

Initially, we imaged tobacco leaves on the 2nd day post infiltration (2 dpi). Additional monitoring was performed on the 3d dpi and surprisingly, we were able to image the actin cytoskeleton in addition to signals from the nucleus for combinations with p35S:SP^{NLS}-GFP-PDZlig.

As shown in Figure 11, at 2 dpi, the fluorescence signal was relatively low and mainly located in nuclei due to the nuclear localizing signal (NLS) in class II construct, indicating that most GFP-PDZlig fusions did not bind to the PDZ domain. We reasoned that the time required for expressing the class I and class II constructs might be different, and in turn the PDZ-PDZlig interaction might occur at a later time point. And indeed, at 3 dpi, the fluorescence intensified when viewed with a stereo-microscope. Using a confocal microscope, distinct filamentous structures resembling F-actins were detected. Among three class I constructs tested, co-infiltration with the 4xPDZ class I construct yielded best results as an F-actin reporter.

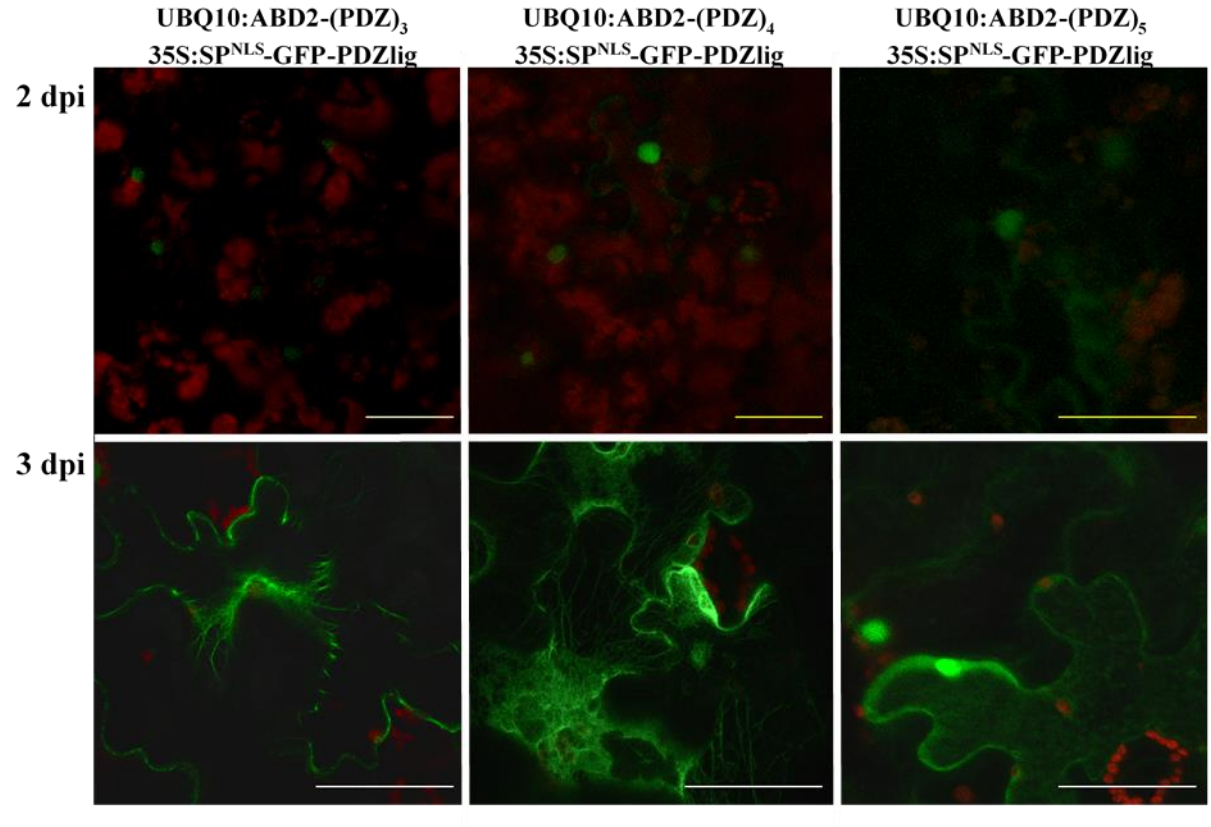

Figure 11. Time-dependent localization of co-infiltration with various class I and the p35S:SP^{NLS}-GFP-PDZlig construct. Confocal images were taken at 2 and 3 dpi. Scale bar = 50μm.

3.3.5. Current approach requires further optimization to increase fluorescence signal

The combinations of class I constructs and p35S:SP^{NLS}-GFP-PDZlig were selected for comparative experiments with the published pUBQ10:GFP-ABD2-GFP reporter. At 3 dpi, distinct F-actin structures were visualized in all three combinations. However, no signal increase was observed in proportion to the copy numbers of PDZ in class I constructs. Instead, brighter signals were mostly recorded with 4xPDZ construct among all three class I constructs. In comparison with the pUBQ10:GFP-ABD2-GFP construct, the new tagging system did not yield signal improvements in the transient assay.

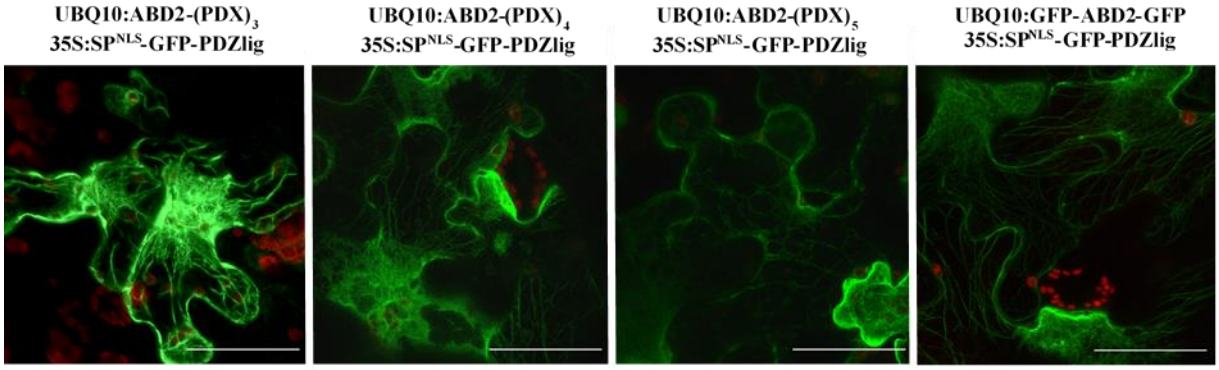

Figure 12. Comparison of our split-tagging system and the pUBQ10:GFP-ABD2-GFP reporter. Different combinations of class I constructs with p35S:SP^{NLS}-GFP-PDZlig, and the pUBQ10:GFP-ABD2-GFP construct were infiltrated in the same tobacco leaf at different locations. All images were taken by confocal microscopy (63x water objective) at 3 dpi. Scale bar = 50μm.

3.3.6. mCherry effects on actin live imaging

According to our original cloning strategy, the class I constructs were supposed to contain one fluorescent protein for referencing the occupancy of GFP from class II constructs. The red fluorescent protein, mCherry was chosen due to its well separated spectra compared with GFP. As preliminary tests, we compared two previously reported F-actin reporter constructs, pUBQ10:GFP-ABD2-GFP and pUBQ10:mCherry-ABD2-mCherry (Dyachok et al., 2014) in transient assays. As shown in Figure 13, mCherry caused actin bundling, which prevented imaging of fine F-actin filaments in our transient assays. Therefore, mCherry was excluded from further cloning processes to avoid complications.

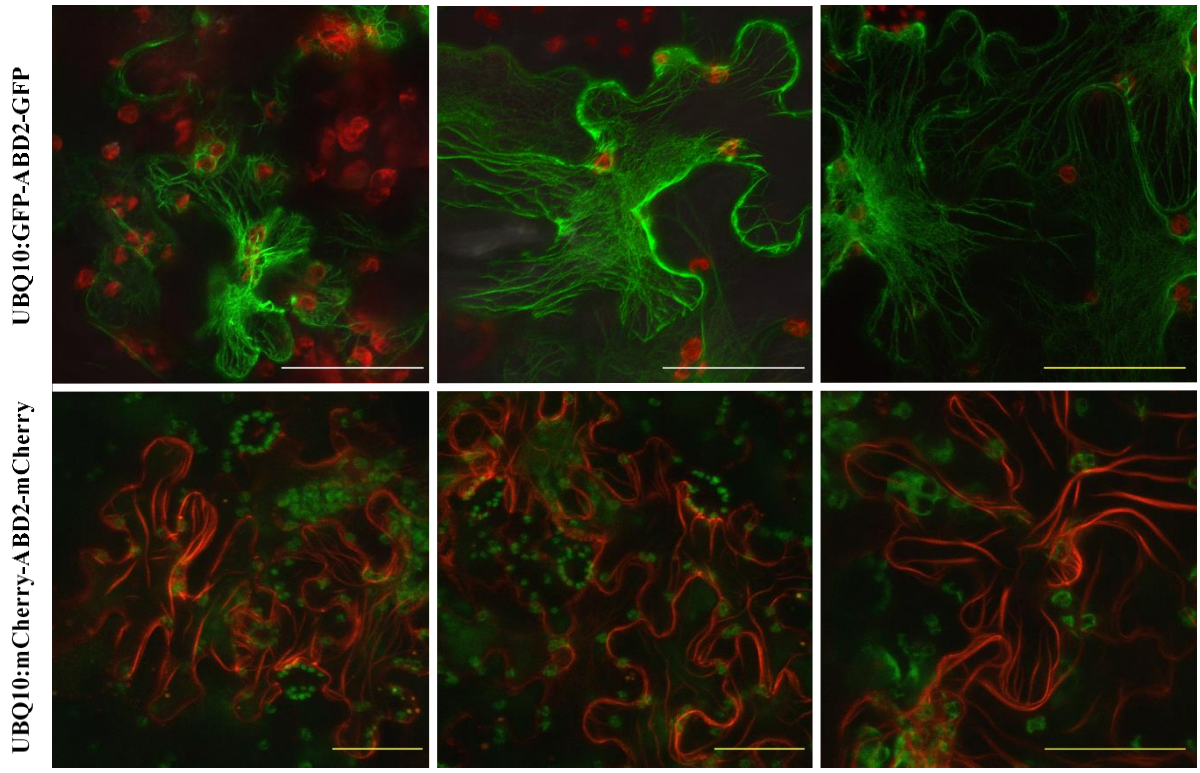

Figure 13. Side-effect of mCherry in transient assays. Images were taken on the third day after infiltration. The first row are images with pUBQ10:GFP-ABD2-GFP construct (GFP signals are shown in green, and chloroplast autofluoresence is shown in red). The second row are images with pUBQ10:mCherry-ABD2-mCherry (mCherry signals are shown in red, and chloroplast autofluorescence in green). All images are taken by confocal microscopy (63x water objective) on the third day after infiltration.

DISCUSSION

In current thesis we described a new approach for development of F-actin reporters in living plant cells. Our method combines two different classes of construct (class I and class II), which were used by co-infiltration in the transient assays for actin imaging.

Multimerization of PDZ requires vector with large input and two-step PCR is a useful tool for assembling small fragments.

Major part of current thesis focused on the establishment of class I and class II constructs by using various molecular cloning methods.

The first attempt to create multiple copies of PDZ in a small cloning vector was inspired mostly by the Golden Gate method (Engler et al., 2008). By using isocaudomers the one tube single reaction permits multimerization of interesting fragments with complementary ends. The reason of low success in our first experiment may have been low concentration of DNA and sub-optimal cycle conditions. In addition, the multimerized PDZ fragment was used to ligate with the small vector pUC57-mini, which was very likely to accommodate inserts below 1kb as suggested by the fact that only up to 3xPDZ (~0.9kb) was cloned into pUC57-mini despite many attempts in this study. The further cloning was thus performed in the big binary vector pCAMBIA1390 (8861kb).

GFP-PDZlig was established by using two-step overlap PCR method. The complementary sequence in one end of both fragments is essential in the second PCR step. This allowed partial annealing between two PCR products from the first step, which in turn served as the template for the second PCR step. In comparison to traditional cut-and-paste method, the overlap PCR is relatively fast since it does not require a ligation and transformation cycle to join two fragments together. However, it does require longer primers to include sufficient overlap between two fragments.

Promoter selection is critical point in construct establishment

Previously it has been shown that F-actin reporters based on the ABD from actin regulatory proteins perturbed actin organization and dynamics and resulted in growth defects (Wang et al., 2004). Furthermore, high expression of fluorescent protein tends to cause strong background, which hinders imaging of certain structures. These side-effects can be minimized by replacing the strong constitutive 35S promoter with the moderate UBQ10 promoter (Wang et al., 2008; Dyachok et al., 2014). In current study, one of the key issues on generating different constructs

was the selection of appropriate promoter. According to the functional roles of class I and class II constructs, the moderate pUBQ10 was selected for class I establishment, and the stronger p35S was chosen for class II constructs. The comparison in transient assays for promoters effects to fluorescence intensity was performed by using UBQ10:GFP-ABD2-GFP and 35S:GFP-ABD2-GFP (Wang et al., 2008; Dyachok et al., 2014) constructs. The difference in signal intensity was evident only by stereo-microscopy, exploiting big area (Figure 8). For future purpose, one possible optimization for our method is using different promoters other than pUBQ10 and p35S.

Signal peptides and time-factor have significant effects

The major function of signal peptides has been shown relatively long time ago (Blobel et al., 1975). Base on the SunTag system, addition of signal peptides in the class II constructs may help to reduce high background. As demonstrated in current study, signal peptide had significant influence in the initial phase of experiment (at 2 dpi) as it determined the localization of GFP.

Results at 2 dpi suggested that the majority of class II fusions did not bind to the PDZ domain in the class I fusions. Due to the use of different promoters (pUBQ10 vs. p35S), we suspected that the time required for expressing the class I and class II constructs might be different and in turn the PDZ-PDZlig interaction only occurred at later time points. In addition, the larger size and the repeated PDZ domains in class I constructs might cause delayed translation and protein instability. To clarify this point, class I and class II constructs can be infiltrated separately with a time lag in the same leaf region. Alternatively, different promoters can be used and tested for transcriptional activities in a time course.

Current split-tagging method is not optimal to influence the fluorescence signal intensity

As shown before, the recruitment of multiple fluorescence protein increased the fluorescence signal intensity (Genové et al., 2005, Wang et al., 2008, Tanenbaum et al., 2014). Relying to previous studies, our established class I constructs included up to 5 copies of PDZ domains, which presumably could have dramatic improvements on the intensity of fluorescence signal. However, no clear difference in signal intensity was found proportionally to the number of PDZ repeats. This strongly suggested that full occupancy on the PDZ domains by GFP fusions was not achieved. One possibility could be the instability of class I fusions due to the repeated PDZ domain. Alternatively, the distance between PDZ domains might lead to space hindrance to

neighboring GFPs. Due to lack of a reference FP in the class I constructs, these issues were not verified in the current study, but will be important in the future modifications.

SUMMARY

Improving live cell imaging methods, which are central for our understanding on actin dynamics and organization in the cell is an important challenge. Especially taking into accounts the essential role of actin in cell signaling cascades responding to dynamical environmental stimuli.

Our split-tagging strategy was inspired mainly by the recent report on development and applications of the SunTag system (Tanenbaum et al., 2014). By using a novel tagging system based on antibody-antigen interaction, the SunTag allowed recruitment of up to 24 GFP monomers to dramatically increase fluorescence output that enables single molecule imaging by confocal microscopy. However, the antibody-based systems generally are limited to problems related to the large size, low expression levels and insolubility of antibodies.

In the current study, we developed an alternative split-tagging system based on interactions between small protein domains and their corresponding ligands. Two separate classes of constructs, each containing one module from the chosen protein-protein interacting pair assemble *in vivo* to recruit multiple GFPs in the reporter system. Various molecular cloning techniques and concepts have been explored to create the constructs. Interestingly, our method is highly dependent on the time factor. Binding between the chosen protein-protein interacting modules mostly occurred at later time points in our transient assays, possibly due to different promoters used in the two separate classes of constructs. No proportional signal enhancement was observed based on the copy numbers of protein interacting domain, which may be caused by sub-optimal spacers between the interacting domain repeats. Altogether, results of current thesis affirmed our method as a useful approach for developing live cell actin reporters albeit optimizations in several aspects are needed.

KOKKUVÕTE

Maare Mõttus

Uute taimse F-aktiini reporterite loomine kasutades

***split-tagging* süsteemi**

Aktiinid on kõrgelt konserveerunud globulaarsed valgud, mis esinevad eukarüootsete organismide rakkudes kahes erinevas vormis – globulaarses ja filamentaarses. Globulaarsed aktiini osakesed ühinevad rangelt reguleeritud protsessi käigus helikaalseteks filamentideks, mis on peamisteks komponentideks tsütoskeleti moodustumisel. Tsütoskeletti võib nimetada ka raku tugiskeletiks, kuna selle najal kujuneb üldine struktuur, viiakse läbi tsütokinees, tsütoplasma tsirkulatsioon ning organellide ümberpaigutamine. Lisaks tagab tsütoskelett rakkude polaarse kasvu, funktsioneerib nii rakusisese kui rakkudevahelise signaaliülekande rajana, kujundades rakulise vastuse keskkonnatingimustele. Ülalöeldust on selge, et aktiinidel on raku seisukohalt elutähtis roll, mille tõttu on uute, minimaalselt kõrvalefekte omavate uurimismeetodite väljatöötamine hädavajalik.

Algselt toimus aktiinide visualiseerimine vaid fikseeritud preparaatidel, kasutades immuunoflorestsentsi meetodit või aktiinidega seonduvat seene toksiini (Krauss et al., 2003; Deeks et al., 2009). Olulise läbimurde visualiseerimise vallas tõi kaasa rohelise florestseeruva valgu (*GFP*) avastamine, mille baasil toimus plahvatuslik uute meetodite arendamine ja kasutuselevõtt. Kõigele vaatamata pole siiani suudetud välja töötada süsteemi, millel puuduksid negatiivsed kõrvalmõjud raku morfoloogiale, metabolismile või kalduvus artefakte tekitada. Seetõttu vajab tehnoloogiate arendamine ning uute lahenduste leidmine veel põhjalikku uurimistööd.

Meie loodud meetod on inspireeritud kahest erinevast lähenemisviisist signaali tugevdamiseks bioloogilistes süsteemides (Dueber 2009; Tanenbaum et al., 2014). Loodud kontseptsioon võimaldab aktiinide visualiseerimist läbi kahte erinevasse klassi kuuluvate sünteetiliste komplekside seostumise valk-valk interaktsiooni kaudu. Mõlemasse klass kuuluvad kompleksid disainiti modifitseeritavateks, võimaldades tulevikus lihtsate kloonimisvõtetega asendada erinevaid komponente.

Käesolevas töös valmistati ja kasutati klass I ja klass II komplekse. Esimesse klassi kuuluvad kompleksid kodeerisid aktiini seostumise domeeni (*ADB2*) ja vastavalt disainile ühte kuni viit PDZ valku kodeeriva regiooni kordust. *ADB2*, täpsemalt aktiini fimbriini domeen, võimaldas

kompleksil seonduda aktiini filamentidega. PDZ valku kodeeriva järjestuse mitmekordistamine oli oluline osa isokautomeersete restriktsiooniensüümide kasutamisel. Klass II kompleksid sisaldasid lisaks roheliselt florestseeruvale valgule veel PDZ ligandi – valku, mis oli võimeline seostuma klass I kompleksi poolt kodeeritud PDZ domeeniga. Mida rohkem oli PDZ domeeni kodeerimisjärjestuse koopiaid klass I kompleksis, seda rohkem seostumiskohti oli klass II komplekside poolt kodeeritud produktidele. Varasematele uuringutele põhinedes võimaldab taoline strateegia florestsentsivalkude lokaalse üldarvu tõstmise kaudu florestsentssignaali tugevdamist (Deeks et al, 2005, Tanenbaum et al., 2014).

Varasemalt on ka näidatud, et sarnaste reportersüsteemide loomisel on kriitiliseks faktoriks promootori valik (Wang, et al., 2008, Dyachok et al., 2014). Meie kasutasime klass I komplekside loomisel keskmise aktiivsusega promootorit ubikvitiin 10 (UBQ10), et vältida aktiiniga seonduvate valkude ületootmisest tingitud häireid aktiin dünaamikas. Klass II komponentide konstrueerimisel eelistasime tugevamat 35S promootorit, mis võimaldas suurendada florestsentsvalkude ekspressiooni.

Käesolevas töös kasutati loodud komplekside taimerakkudesse sisestamiseks agro-koosinfiltreerimise meetodil ehk mõlema klassi komplekside hulgast valiti üks ning infiltreeriti need tubaka *Nicotiana benthamiana* lehtedesse. Kokku uuriti üheksat erinevat kombinatsiooni klass I ja klass II kompleksidest, mille kodeeritud produktid ühinesid rakkudes valk-valk (PDZ-PDZ ligand) seostumise kaudu.

Uurimise tulemused viitavad otseselt antud süsteemi tundlikkusele ajafaktori suhtes. Potentsiaalne põhjus võis seisneda klass I ja klass II komplekside ekspressioonitaseme erinevuses tulenevalt promootorite aktiivsuse ja lisaks lõpp-produktide pikkuse varieeruvusest eri klassi komplekside lõikes.

Eksperimentaalselt leidis kinnitust, et loodud meetod on kasutatav aktiini filamentide visualiseerimiseks elusates rakkudes. Meie loodud meetod vajab tulevikus täiendavat optimeerimist, võimaldamaks fluorestsentssignaali regulatsiooni.

LITERATURE CITED

Binz, H.K., Amstutz, P., Kohl, A., Stumpp, M.T., Briand, C., Forrer, P., Grütter, M.G., and Plückthun, A. (2004) High-affinity binders selected from designed ankyrin repeat protein libraries. Nat Biotechnol, 22, (5), 575-582.

Blancaflor, E.B., and Gilroy, S. (2000) Plant cell biology in the new millennium: new tools and new insights. Americ J of Bot, 87(11), 1547-1560.

Bugyi, B., and Carlier, M.F. (2010) Control of actin filament treadmilling in cell motility. Annu Rev Biophys, 39, 449-470.

Chalfie, M., Tu, Y., Euskirchen, G., Ward, W.W., and Prasher, D.C. (1994) Green fluorescent protein as a marker for gene expression. Science, 263, (5148), 802-805.

Collings, D.A., and Wasteneys, G.O. (2005) Actin microfilament and microtubule distribution patterns in the expanding root of *Arabidopsis thaliana*. Can J Bot, 83(6), 579-590.

Deeks, M.J., and Hussey, P.J. (2009) Plant actin biology. ELS, John Wiley and Sons, Ltd: Chichester, 1-8.

Dominguez, R., and Holmes, K.C. (2011) Actin structure and function. Annu Rev Biophys, 40, 169-186.

Drøbak, B.K., Franklin-Tong, V.E., and Staiger, C.J. (2004) The role of the actin cytoskeleton in plant cell signaling. New Phytol, 163(1), 13-30.

Dueber, J.E., Wu, G.C., Malmirchegini, G.R., Moon, T.S., Petzold, C.J., Ullal, A.V., Prather, K.L., and Keasling, J.D. (2009) Synthetic protein scaffolds provide modular control over metabolic flux. Nat Biotechnol, 27, (8), 753-759.

Dyachok, J., Sparks, J.A., Liao, F., Wang, Y.S,. and Blancaflor, E.B. (2014) Fluorescent protein-based reporters of the actin cytoskeleton in living plant cells: fluorophore variant, actin binding domain, and promoter considerations. Cytoskeleton (Hoboken), 71(5), 311-327.

Engler, C., and Marillonnet, S. (2014) Golden Gate cloning. Methods Mol Biol, 1116, 119-131.

Engler, C., Gruetzner, R., Kandzia, R., and Marillonnet, S (2009) Golden Gate shuffling: A one-pot DNA shuffling method based on type IIs restriction enzymes. PLoS ONE, 4, (5), e5553.

Fleischmann, M., Bloch, W., Kolossov, E., Andressen, C., Müller, M., Brem, G., Hescheler, J., Addicks, K., and Fleischmann, B.K. (1998) Cardiac specific expression of the green fluorescent protein during early murine embryonic development. FEBS Lett, 440, (3), 370-376.

Genové, G., Glick, B.S., and Barth, A.L. (2005) Brighter reporter genes from multimerized fluorescent proteins. BioTechniques, 39, 814-822.

Gong, S., Zheng, C., Doughty, M.L., Losos, K., Didkovsky, N., Schambra, U.B., Nowak, N.J., Joyner, A., Leblanc, G., Hatten, M.E., and Heintz, N. (2003) A gene expression atlas of the central nervous system based on bacterial artificial chromosomes. Nature, 425, 917-925.

Hussey, P.J., Ketelaar, T., and Deeks M.J. (2006) Control of the actin cytoskeleton in plant cell growth. Annu Rev Plant Biol, 57, 109-125.

Ketelaar, T., Anthony, R.G., and Hussey, P.J. (2004) Green fluorescent protein-mTalin causes defects in actin organization and cell expansion in *Arabidopsis* and inhibits actin depolymerizing factor's actin depolymerizing activity *in vitro*. Plant physiol, 136, (4), 3990-3998.

Kost, B., Spielhofer, P., and Chua, N-H. (1998) A GFP-mouse talin fusion protein labels plant actin filaments *in vivo* and visualizes tha actin cytoskeleton in growing pollen tubes. Plant J, 16, 393-401.

Krauss, S., Chen, C., Penman, S., and Heald, R. (2003). Nuclear actin and protein 4.1: essential interactions during nuclear assembly *in vitro*. Proc Natl Acad Sci USA, 100, 10752–10757.

Kreplak, L., Fudge, D. (2007). Biomechanical properties of intermediate filaments: from tissues to single filaments and back. Bioessays, 29, 26–35.

Liu, J.-Z., Blancaflor, E.B., and Nelson, R.S. (2005) The tobacco mosaic virus 126 kD protein, a constituent of the virus replication complex, alone or within the complex aligns with and traffics along microfilaments. Plant Physiol, 138,1853–1865.

Lloyd, C.W. (1987) The plant cytoskeleton: the impact of fluorescence microscopy. Annu Rev Plant Physiol, 38, 119–139.

Marc, J., Granger, C.L., Brincat, J., Fisher, D.D., Kao, T.H., McCubbin, A.G., and Cyr, R.J. (1998) A GFP-MAP4 reporter gene for visualizing cortical microtubule rearrangements in living epidermal cells. Plant Cell, 10, 1927-1940.

McKayed, K.K., and Simpson, J.C. (2013) Actin in action: imaging approaches to study cytoskeleton structure and function. Cells, 2, (4), 715-731.

Nick, P. (1999) Signals, motors, morphogenesis – the cytoskeleton in plant development. Plant Biology, 1, 169–179.

Pantaloni, D., Clainche, C.L., and Carlier, M.-F. (2001) Mechanism of actin-based motility. Science, 292, (5521), 1502-1506.

Remedios, C.G.D., Chhabra, D., Kekic, M., Dedova, I.V., Tsubakihara, M., Berry, D.A., and Nosworthy, N.J. (2002) Actin binding proteins: regulation of cytoskeletal microfilaments. Physiol Rev, 83, (2), 433-473.

Ren, H., Gibbon, B.C., Ashworth, S.L., Sherman, D.M., Yuan, M., and Staiger, C.J. (1997) Actin purified from maize pollen functions in living plant cells. Plant Cell, 9(8), 1445-1457.

Sano, T., Higaki, T,. Oda, Y., Hayashi,T., and Hasezawa, S. (2005) Appearance of actin microfilament 'twin peaks' in mitosis and their function in cell plate formation, as visualized in tobacco BY-2 cells expressing GFP-fimbrin. Plant J 44, 595–605.

Schmit, A.C., and Lambert, A.M. (1990) Microinjected fluorescent phalloidin *in vivo* reveals the F-actin dynamics and assembly in higher plant mitotic cells. Plant Cell, 2(2), 129-138.

Sheahan, M.B., Staiger, C.J., Rose, R.J., and McCurdy, D.W. (2004) A green fluorescent protein fusion to actin-binding domain 2 of *Arabidopsis* fimbrin highlights new features of dynamic actin cytoskeleton in live plant cells. Plant Physiol, 136, (4), 3968-3878.

Tanenbaum, M.E., Gilbert L.A., Qi, A.S., Weissman, J.S., and Vale, R.D. (2014) A protein-tagging system for signal amplification in gene expression and fluorescence imaging. Cell, 159, 635-646.

Wang, Y.S., Motes, C.M., Mohamalawari, D.R., and Blancaflor, E.B. (2004) Green fluorescent protein fusions to *Arabidopsis* fimbrin 1 for spatio-temporal imaging of F-actin dynamics in roots. Cell Motil Cytoskeleton, 59, (2), 79-93.

Wang, Y.S., Yoo, C.M., and Blancaflor, E.B. (2008) Improved imaging of actin filaments in transgenic *Arabidopsis* plants expressing a green fluorescent protein fusion to the C- and N-termini of the Fimbrin actin-binding domain 2. New Phytol, 177, (2), 525-536.

Yoo, C.M., Quan, L., Cannon, A.E., Wen, J., and Blancaflor, E.B. (2012) AGD1, a class 1 ARF-GAP, acts in common signaling pathways with phosphoinositide metabolism and the actin cytoskeleton in controlling *Arabidopsis* root hair polarity. Plant J, 69, (6), 1064-1076.

Timmers, A.C.J., Niebel, A., Balagué, C., and Dagkesamanskaya, A. (2002) Differential localisation of GFP fusions to cytoskeleton-binding proteins in animal, plant, and yeast cells. Protoplasma, 220, 69-78.

Schnell, U., Dijk, F., Sjollema, K.A., and Giepmans B.N.G. (2012) Immunolabeling artifacts and the need for live-cell imaging. Nat Methods, 9(2), 152-158.

Used web addresses

- https://www.neb.com/search?q=restriction+enzymes New England Biolabs
- http://www.thermoscientific.com/en/home.html Thermo Scientific

SUPPLEMENTS

1. Restriction enzymes

Table 2. Restriction enzymes and their restriction sites.

Name	Restriction site	Name	Restriction site
BamHI	5′...GGATCC...3′ 3′...CCTAGG...5′	PstI	5′...CTGCAG...3′ 3′...GACGTC...5′
BstEII	5′...GGTNACC...3′ 3′...CCANTGG...5′	SalI	5′...GTCGAC...3′ 3′...CAGCTG...5′
BglII	5′...AGATCT...3′ 3′...TCTAGA...5′	SpeI	5′...ACTAGT...3′ 3′...TGATCA...5′
EcoRI	5′...GAATTC...3′ 3′...CTTAAG...5′	SmaI	5′...CCCGGG...3′ 3′...GGGCCC...5′
HindIII	5′...AAGCTT...3′ 3′...TTCGAA...5′	XbaI	5′...TCTAGA...3′ 3′...AGATCT...5′
NcoI	5′...CCATGG...3′ 3′...GGTACC...5′		

Fast digest restriction enzymes, 10X fast digest buffer, T4 DNA ligase, T4 DNA ligase buffer (10X), DreamTaq buffer (10x), ATP (10mM) were manufactured by Thermo Scientific. DNA polymerase Taq FirePol was manufactured by Solis Biodyne. and GeneRuler by Fermentas. (Restriction enzymes sites were taken from New England Labs website)

Lihtlitsents lõputöö reprodutseerimiseks ja lõputöö üldsusele kättesaadavaks tegemiseks

Mina (*autori nimi*): Maare Mõttus

(sünnikuupäev: 24.01.1992)

annan Tartu Ülikoolile tasuta loa (lihtlitsentsi) enda loodud teose (*lõputöö pealkiri*),

Development of new plant F-actin reporters by a split-tagging system

1. mille juhendaja on: Yuh-Shuh Wang,

1.1. reprodutseerimiseks säilitamise ja üldsusele kättesaadavaks tegemise eesmärgil, sealhulgas digitaalarhiivi DSpace-is lisamise eesmärgil kuni autoriõiguse kehtivuse tähtaja lõppemiseni;

1.2. üldsusele kättesaadavaks tegemiseks Tartu Ülikooli veebikeskkonna kaudu, sealhulgas digitaalarhiivi DSpace´i kaudu alates **25.05.2015** kuni autoriõiguse kehtivuse tähtaja lõppemiseni.

2. olen teadlik, et nimetatud õigused jäävad alles ka autorile.

3. kinnitan, et lihtlitsentsi andmisega ei rikuta teiste isikute intellektuaalomandi ega isikuandmete kaitse seadusest tulenevaid õigusi.

Tartus, _____ (*kuupäev*)